CONTROL OF ENERGETIC PARTICLE RELATED INSTABILITIES IN BURNING PLASMA

S.E. Sharapov

UKAEA, Culham Science Centre, Abingdon OX14 3DB, UK

Acknowledgment: help from M. Van Zeeland in preparing this talk is highly appreciated.

OUTLINE

- INTRODUCTION: WHAT TO EXPECT IN BURNING PLASMAS
- CONTROL OF ENERGETIC PARTICLE RADIAL PROFILE
- SUPRESSION OF ALFVÉN EIGENMODES IN REVERSED-SHEAR DISCHARGES WITH ECRH
- ECRH AND ECCD EFFECTS ON TOROIDAL ALFVÉN EIGENMODES
- SUPPRESSION OF NBI-DRIVEN MODES BY HIGH HARMONIC ICRF ON NSTX-U
- SUMMARY

INTRODUCTION

α-HEATING DOMINATES IN BURNING PLASMA

- **Burning plasmas: auxiliary heating used, but more significant plasma self-heating is by fusion alphas → plasma becomes exothermic medium**

- **The leading-order alpha-heating effects may be identified in accordance with $Q=P_{FUS}/P_{IN}$,**

$Q \approx 1$ – at the threshold (JET had $Q \approx 0.6$ in record fusion power DT plasma)
$Q \approx 5$ – alpha-effects on heating profile and Alfvén instabilities
$Q \approx 10$ – nonlinear coupling between alphas, MHD stability, bootstrap current, turbulent transport, interaction plasma-boundary (ITER target)
$Q \geq 20$ – burn control and transient ignition phenomena
$Q \to \infty$ - ignition

- **Control of burning plasma in the presence of more powerful actor – α-particles can hardly rely on a single "power knob", more intelligent approaches are needed.**

GENERAL THOUGHTS ON CONTROL

- The focus of the techniques must be on essential EP parameters: radial gradients and possible bump-on-tail regions in the velocity space
- In the case of resonant wave-particle interaction the focus should be on small but very sensitive regions of EP phase space around the resonances
- EP-driven instabilities can be controlled via manipulating equilibrium profiles for increased damping of the relevant modes, e.g. increase of continuum damping for TAE case. This involves thermal plasma optimisation.
- A search for several possible control “knobs” is essential. The use of auxiliary power knob alone is rarely effective as nearly maximum power is used anyway.
- In practice, actuators affect multiple mechanisms, e.g. ECCD aiming at q-profile change, changes plasma pressure etc.

CONTROL OF RADIAL PROFILE OF ENERGETIC IONS

Wave-Induced Energetic Particle Pinch Driven by Toroidally Asymmetric ICRF Waves

L.-G.Eriksson et al., Phys. Rev. Lett 81 (1998) 1231
M.J.Mantsinen et al., Phys. Rev. Lett. 89 (2002) 115004

ION CYCLOTRON RESONANCE HEATING

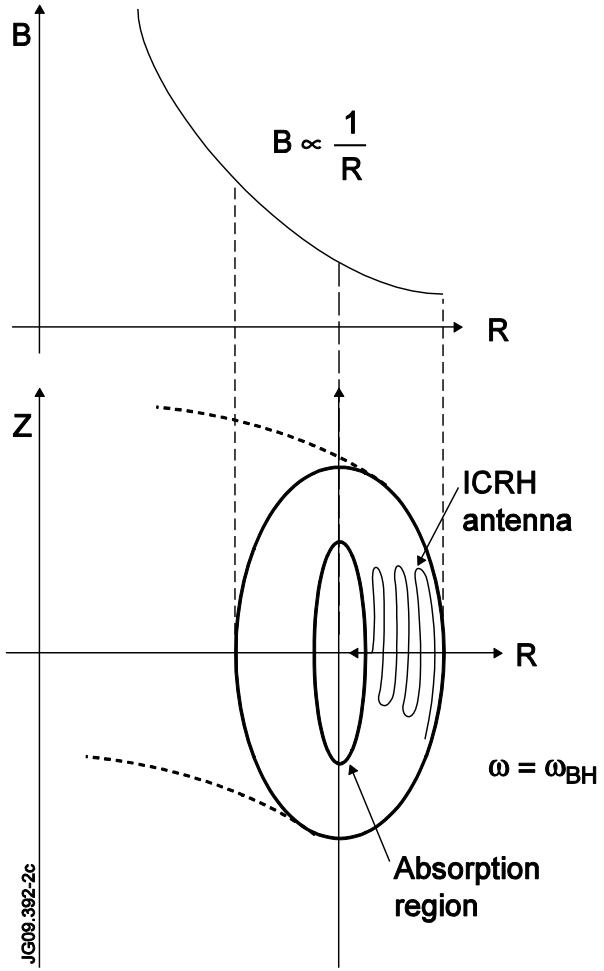

ESSENTIAL WAVE-PARTICLE INVARIANT

- **The *unperturbed* orbit of a particle is determined by three invariants:**

$$\mu \equiv \frac{Mv_\perp^2}{2}; \qquad E \equiv \frac{Mv^2}{2}; \quad P_\varphi \equiv -\frac{e}{c}\psi(r) + RMv_\varphi$$

- **In the presence of a *single EM* mode with wave field $\propto \exp i(n\varphi - \omega t)$, where *n* is toroidal mode number, the wave-particle interaction is invariant with respect to transformation**

$$t \to t + \tau; \quad \varphi \to \varphi + \frac{\omega}{n}\tau$$

- **This implies that though in the presence of ICRF wave, neither E nor P_φ is conserved for interacting ion orbit, *their following combination is still invariant*:**

$$E - \frac{\omega}{n}P_\varphi = const$$

- **Change in the particle energy is related to change in particle radius then**

$$\Delta E = \frac{\omega}{n}\Delta P_\varphi \cong \frac{\omega e}{nc}\psi'\Delta r$$

and it depends on the sign of *n* !
TOROIDALLY PROPAGATING ICRF WAVES

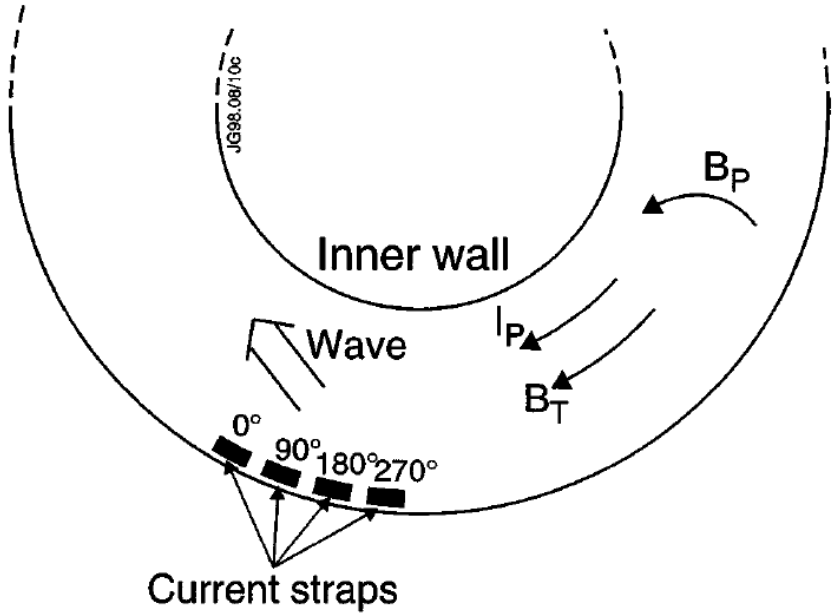

FIG. 1. Schematic view of the JET tokamak seen from above. The directions of the plasma current I_P, toroidal field B_T, poloidal field B_P, and the launched wave in the case of +90° phasing are shown.

THE RADIAL PINCH EFFECT

- **Depending on the phase shift in RF antenna current straps, we can launch wave co-propagating with plasma current ($n>0$, $+90^0$) or counter-propagating ($n<0$, -90^0).**

- **Since the energy of resonating ion increases, we obtain the change in P_φ**

$$\Delta P_\varphi = (n/\omega)\, \Delta E$$

determined by the sign of n.

- **Depending on the sign of n, the population of ICRF-accelerated fast ions becomes either more peaked in radius ($+90^0$ phasing) or more flat (-90^0).**

Evidence for a Wave-Induced Particle Pinch in the Presence of Toroidally Asymmetric ICRF Waves (1998)

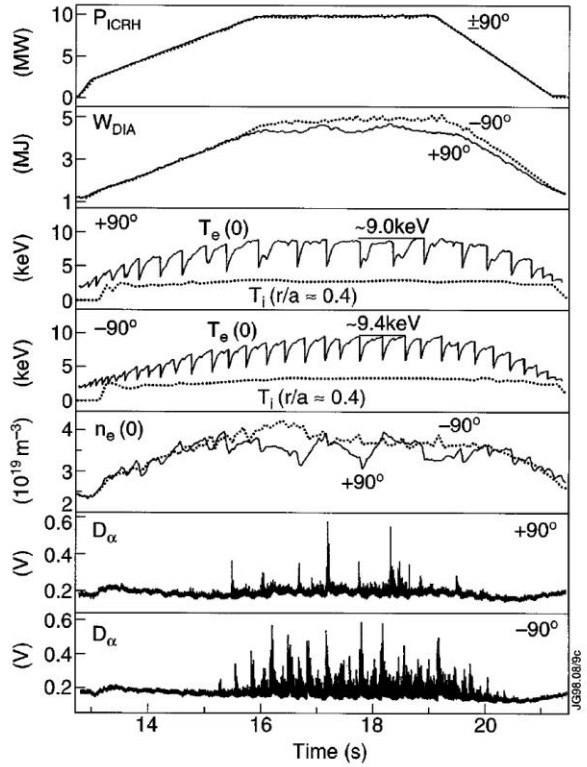

FIG. 2. ICRF power, diamagnetic plasma energy, central electron temperature, ion temperature at $r/a \approx 0.4$, central electron density, and D_α signal for two JET discharges with $+90°$ and $-90°$ phasings (discharges 41 514 and 41 515).

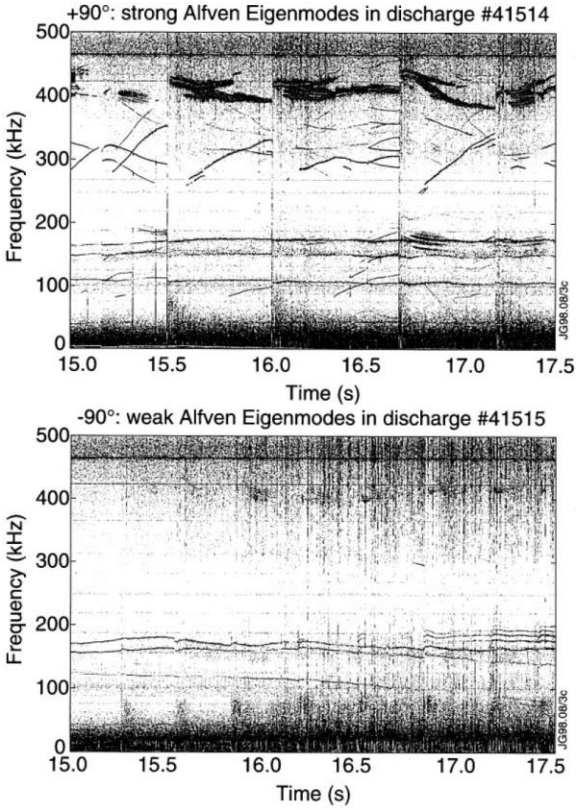

FIG. 3. Spectrograms of MHD activity.

Modelling of fast ion distributions in the two comparison pulses

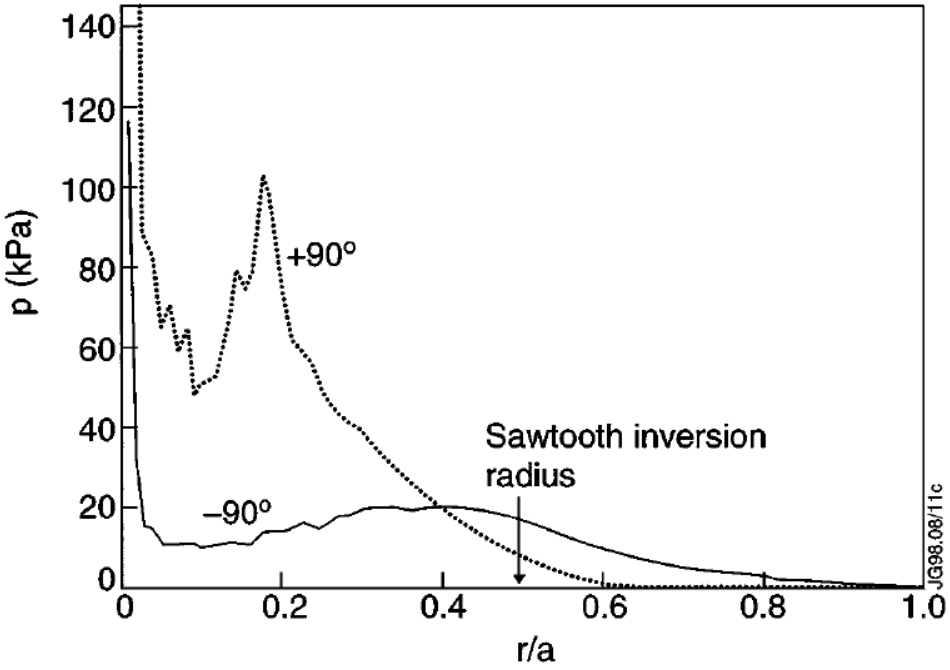

FIG. 6. Simulated fast ion pressure profiles.

Controlling the Profile of Ion-Cyclotron-Resonant ^{3}He Ions in JET with the Wave-Induced Pinch Effect (2002)

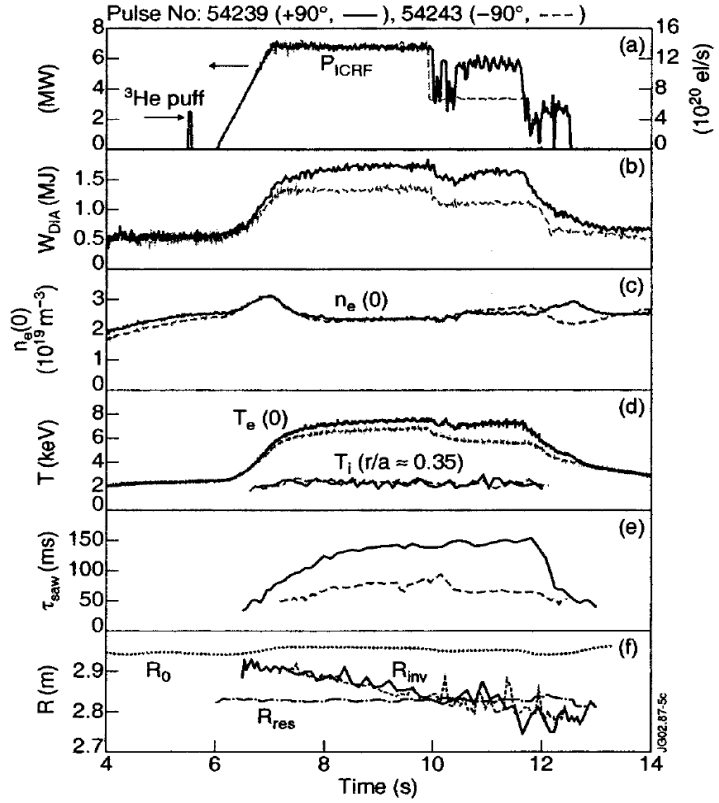

FIG. 1. Overview of two 3.45T/1.8 MA JET ^{4}He discharges with ^{3}He minority heating using +90° and −90° phasings.

Fast ion profiles were measured with 2D γ-ray camera from γ-ray emission from nuclear reaction $^{12}C(^{3}He, p\gamma)^{14}N$ between ICRF-accelerated ^{3}He ions and C impurity

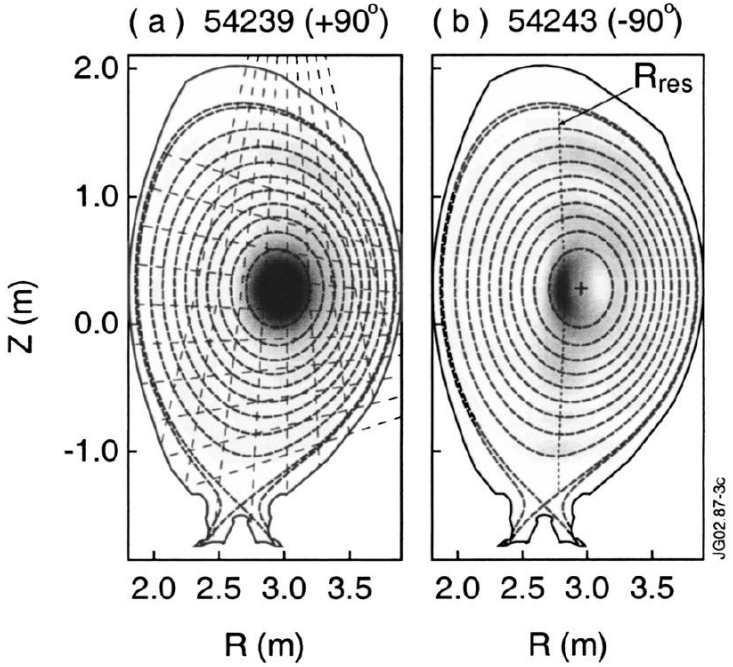

FIG. 2. Contour plots of the reconstructed γ-ray emission profile, normalized to the peak emissivity. The lines of sight of the neutron profile monitor are shown in (a) and the ICRF resonance location in (b).

Mitigation of Alfvén Activity in a Tokamak by Externally Applied Static 3D Fields

A.Bortolon et al., PRL 110, 265008 (2013)

NSTX DISCHARGES WITH BEAM-DRIVEN AEs

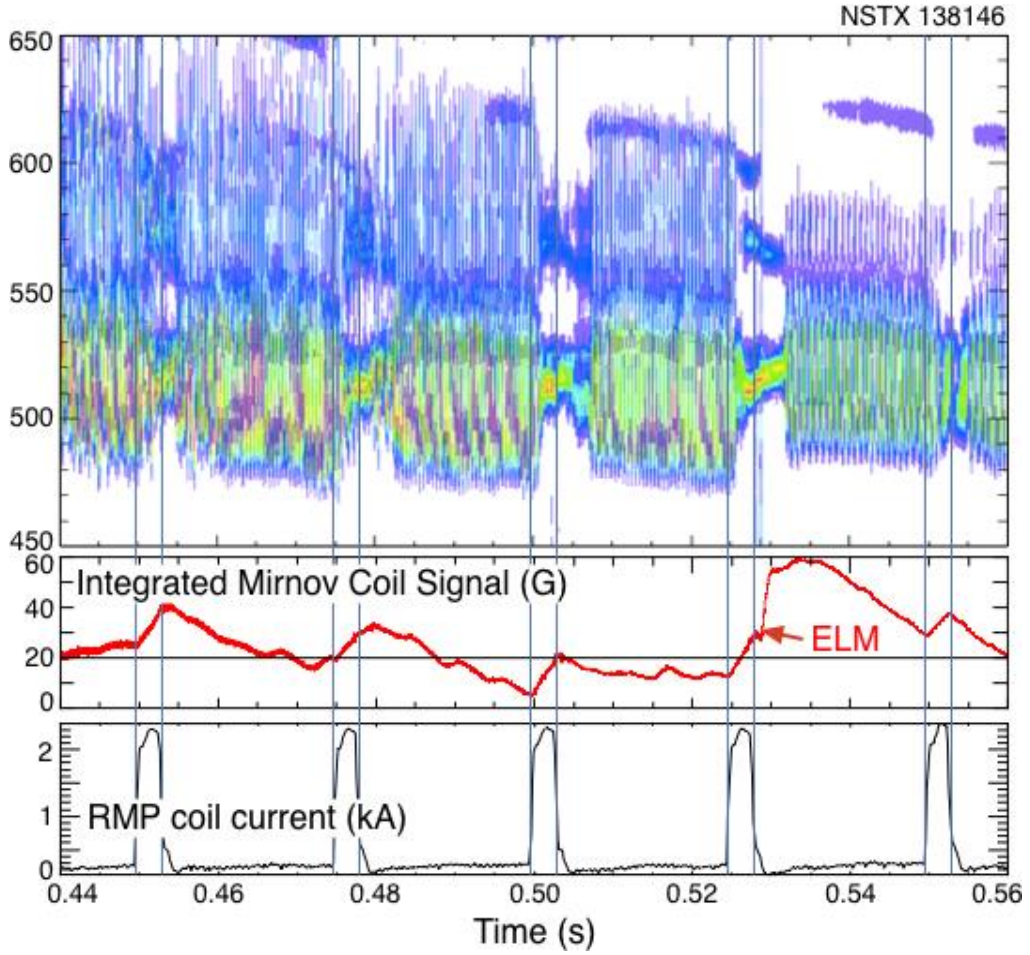

ZOOM OF THE OBSERVATIONS:

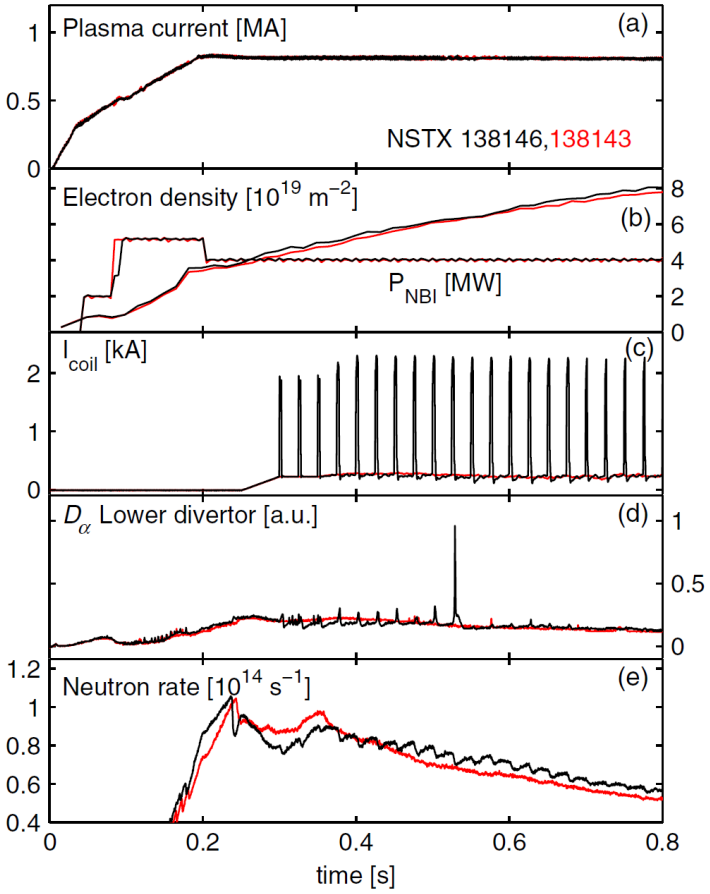

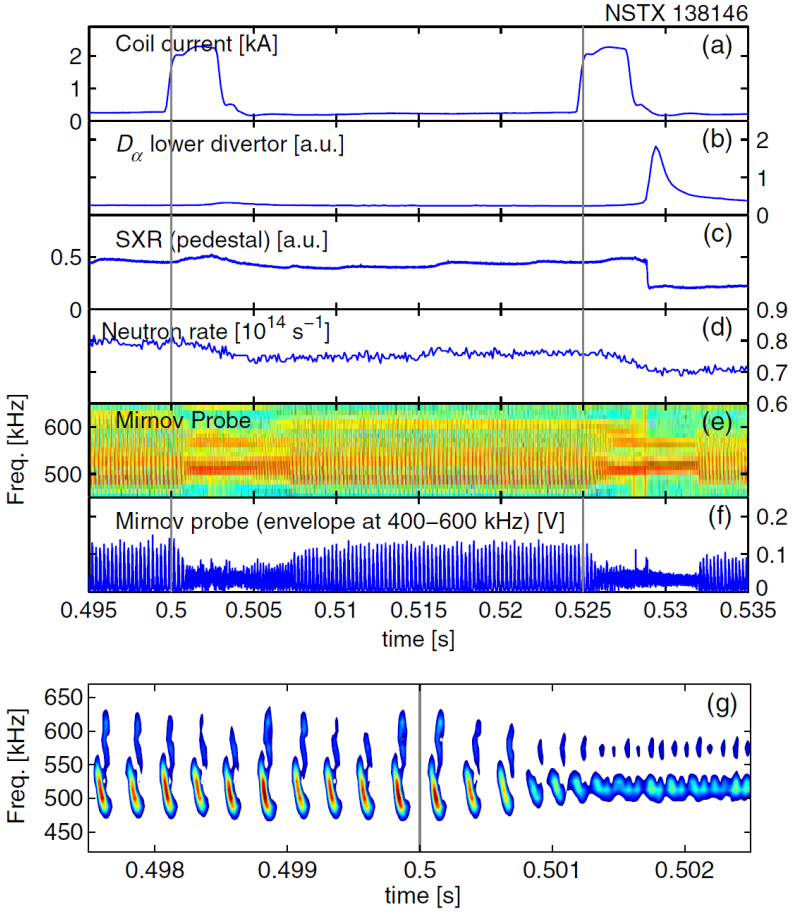

FAST ION POPULATION FALLS BY ≈15% AT THE RESONANCE

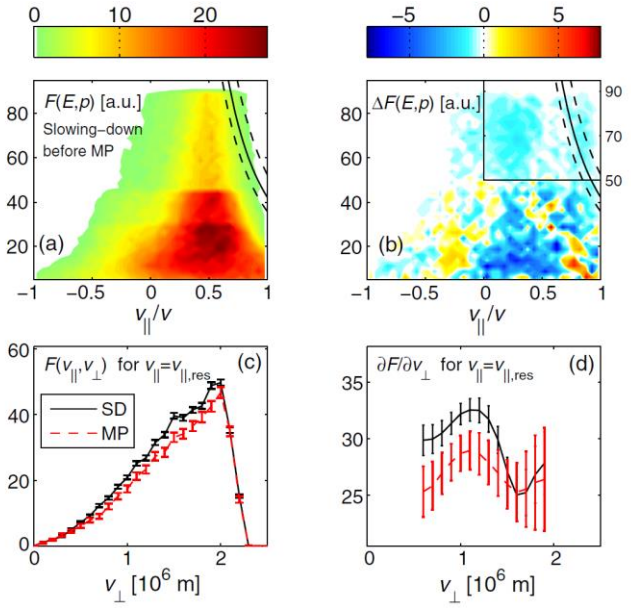

FIG. 5 (color online). Velocity space representation of the slowing-down (SD) distribution function $F(E, p)$ in the plasma core, as computed by SPIRAL (a) before the MP and (b) its variation after 1 ms from the application of the MP including plasma response. The curves overplotted indicate loci of possible resonance between fast ions and a mode at 520 ± 40 kHz. Lower values of F and $\partial F/\partial v_\perp$ along the resonance curve are found in the presence of MP (c), (d). Data in (c), (d) and in the inset of (b) are from simulations with enhanced statistical accuracy.

SUPRESSION OF AEs IN REVERSED-SHEAR DISCHARGES WITH ECRH

REVERSED-SHEAR AE SUPPRESSION BY ECRH ON DIII-D

M. Van Zeeland et al., PPCF 50 (2008) 035009

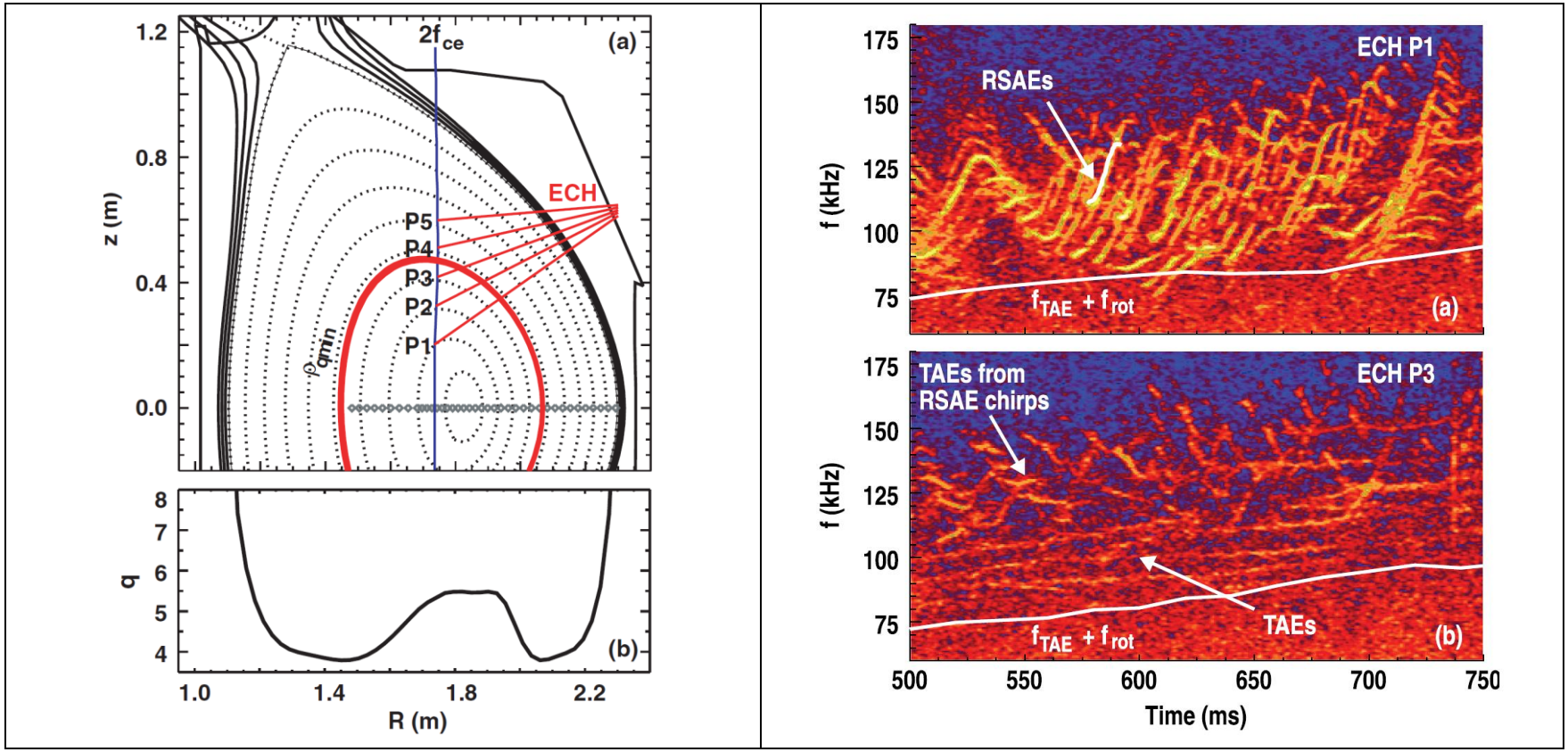

INTERPRETATION: THE AC FREQUENCY BAND BETWEEN GAMs AND TAEs *SHRINKS* AS PRESSURE AND PRESSURE GRADIENT INCREASE

$$f_{GAM} \cong \frac{1}{2\pi}\left(\frac{2}{M_i R_0^2}\left[T_e + \frac{7}{4}T_i\right]\right)^{1/2} \le f_{AC} \le f_{TAE} \cong \frac{V_A}{4\pi q R_0}$$

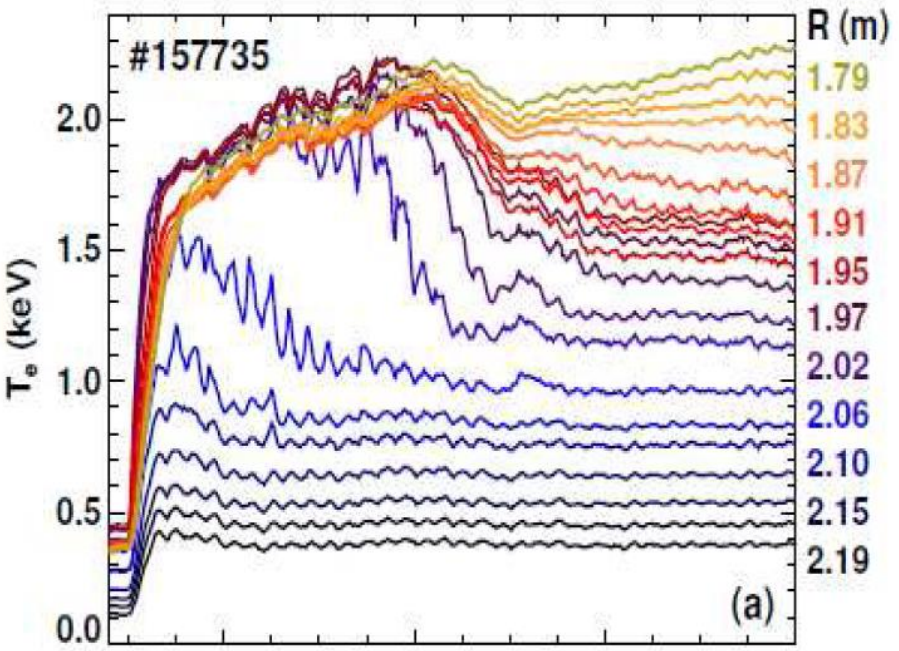

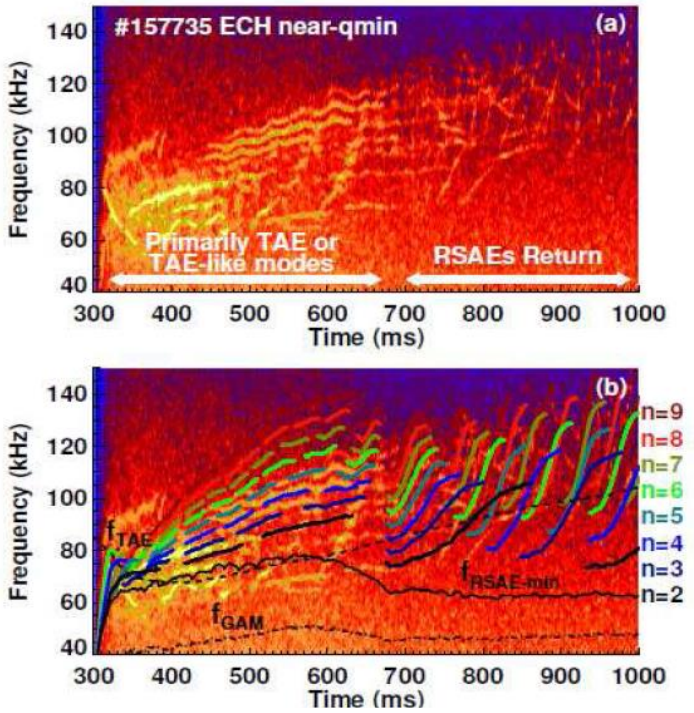

M.A.Van Zeeland et al., Nucl. Fusion 56 (2016) 112007

SIMILAR EXPERIMENT WAS PEFFORMED ON AUG

M.Garcia-Munoz et al. (2018)

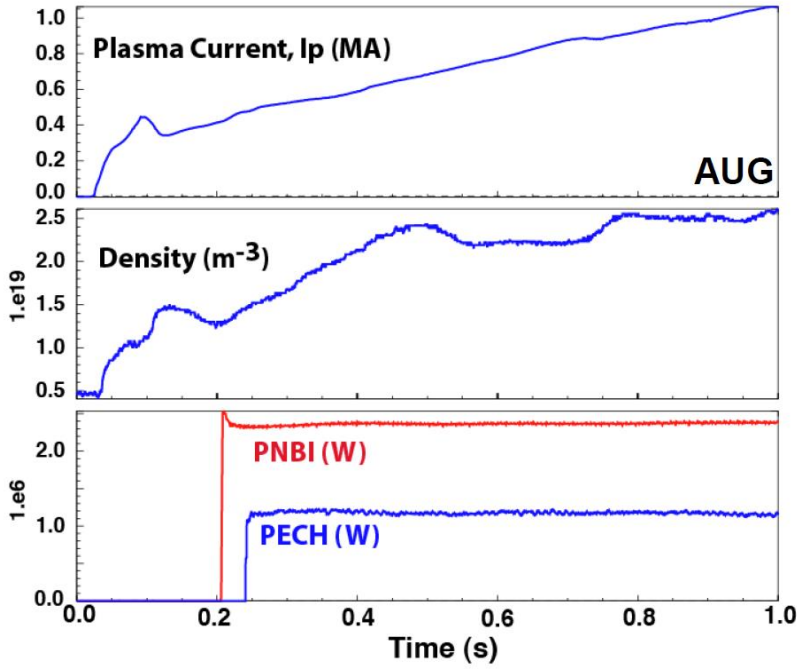

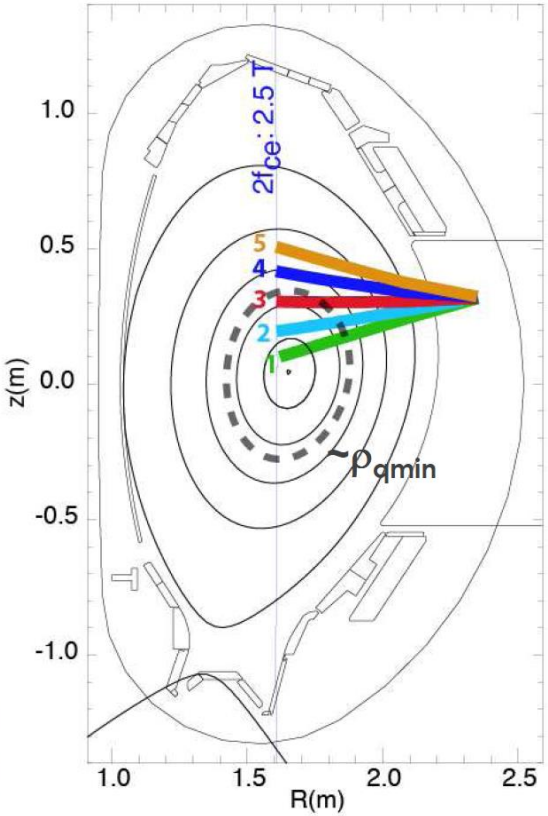

- Beam (60kV) and ECRH heating begin t~0.2s
- ECH deposition location scanned in series of discharges (positions 1-5)

COMPLETE SUPPRESSION OF SIMILAR MODES WAS ACHIEVED

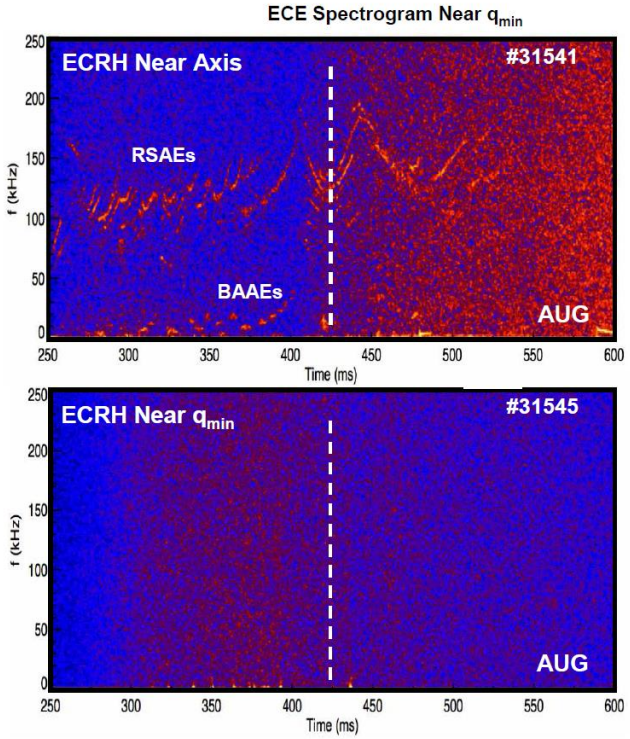

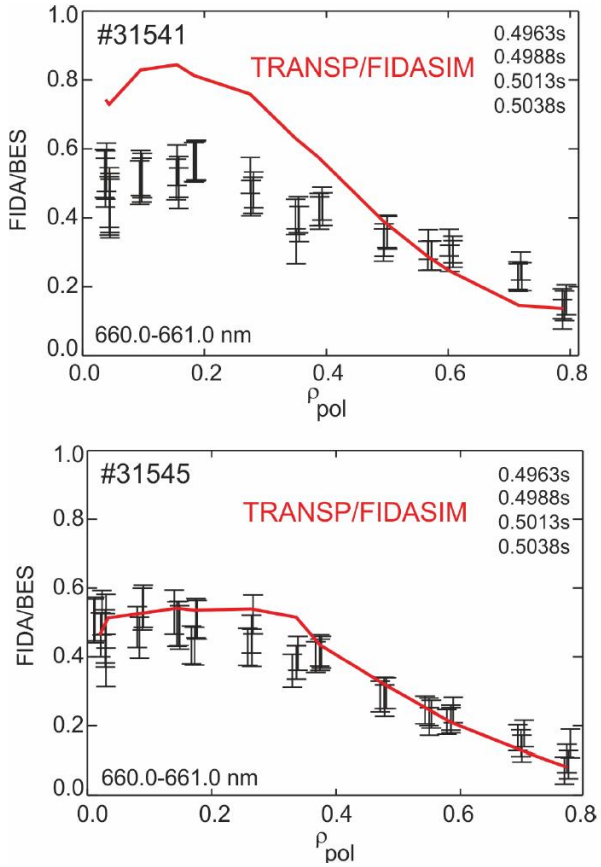

SIMILAR EFFECTS HAVE SINCE BEEN REPRODUCED ON TJ-II, LHD, Heliotron-J, and KSTAR:

1. Nagaoka K. et al 2013 Nucl. Fusion 53 072004

2. Nagasaki K. et al 2012 IAEA FEC, EX/P8-10

3. Kim J. 2018 APS DPP

This effect was then perfected on DIII-D and active real-time control of AEs by NBI and ECH was demonstrated !

W.Hu et al 2018 Nucl. Fusion 58 124001

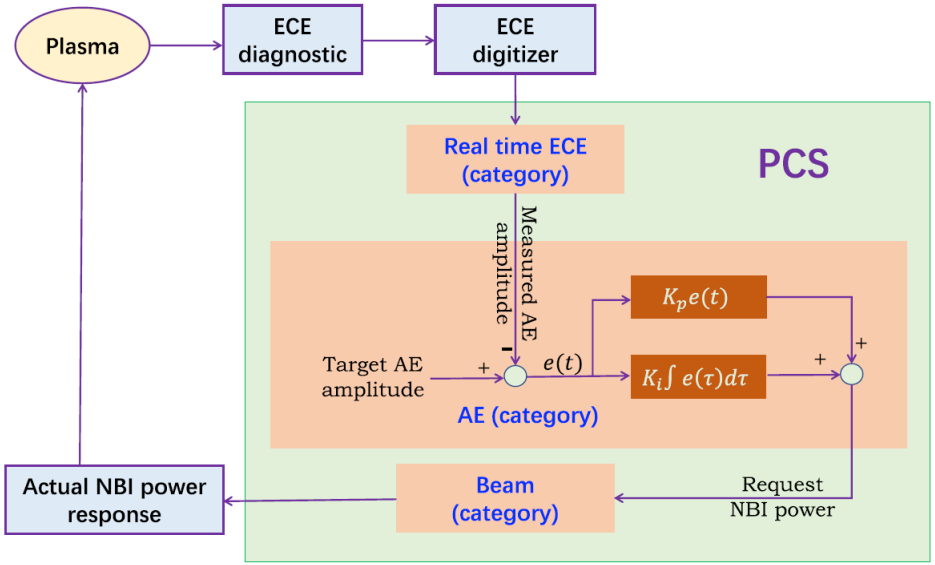

Figure 2. Diagram of the proportional-integral AE control system in the DIII-D PCS. 'Category' refers to different functional areas in the PCS software architecture that enable both operators and control designers to organize control operations by relevant actuators, diagnostics, or control goals.

TESTING THE MODE RESPONSE TO NBI POWER MODULATION

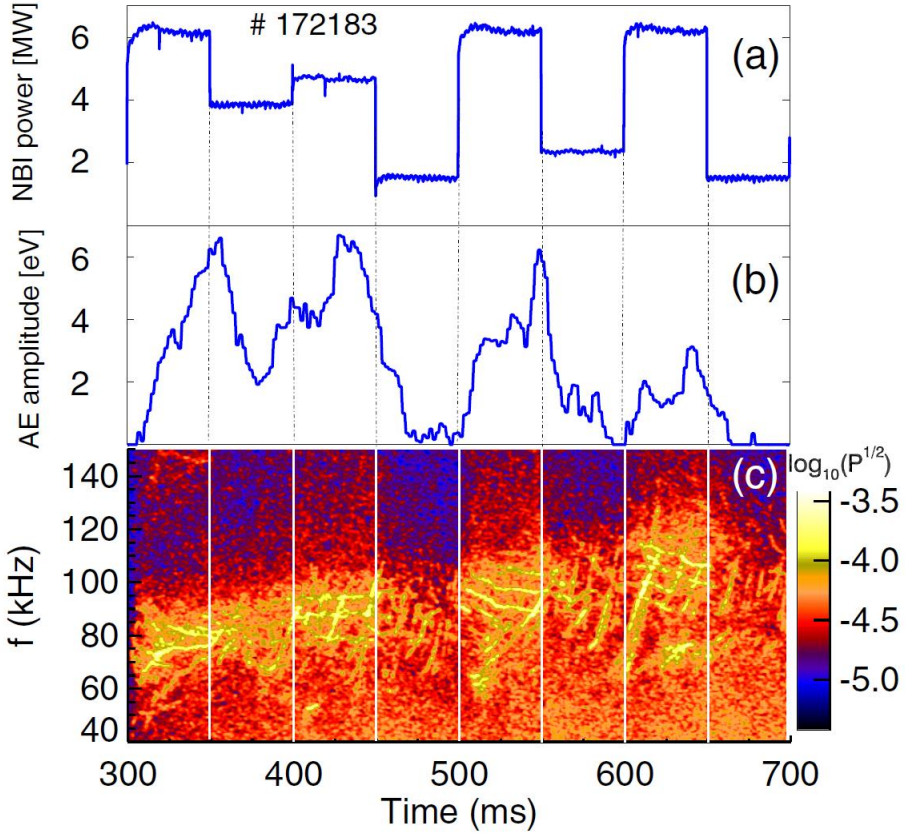

Figure 3. Discharge 172183. (*a*) Pre-programmed NBI power, (*b*) AEs amplitude represented by electron temperature measured by ECE, (*c*) CO_2 interferometer cross power spectrum.

EXAMPLE OF THE NBI POWER CONTROLLED BY AE AMPLITUDE

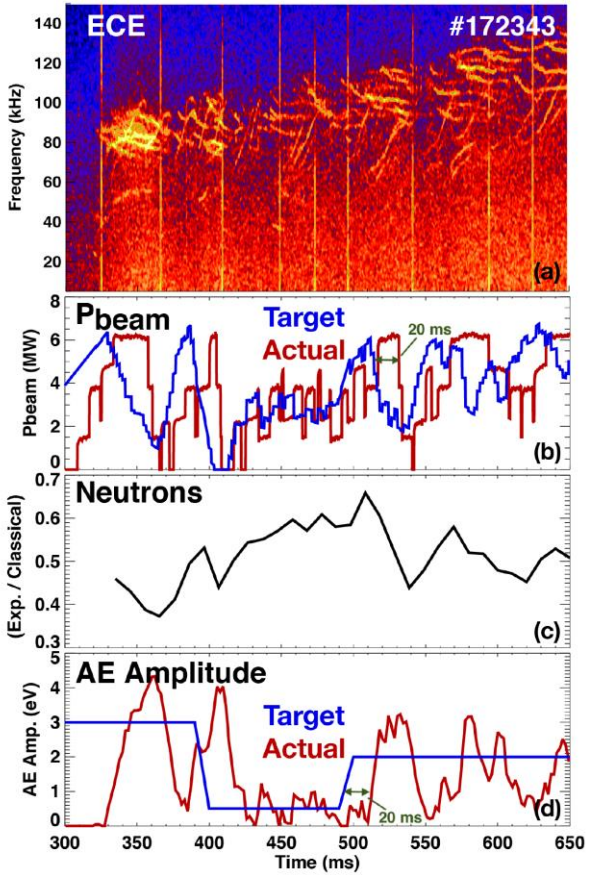

Figure 4. Discharge 172343. (*a*) ECE spectrum, (*b*) AE controller requested NBI power (blue line) and actual response NBI power (red line), (*c*) measured neutrons production rate over TRANSP predicted classical neutrons production rate and (*d*) target AE amplitude (blue line) and real-time ECE measured AE amplitude (red line).

FORWARD TO ECRH/ ECCD EFFECTS ON TAEs

(More ITER relevant)

THE IDEA OF ECRH/ ECCD EFFECT ON TAE IN ITER

ECRH/ECCD may be applied in a *prescribed narrow region* in order to form a *TAE-free transport barrier* preventing radial transport of alpha-particles

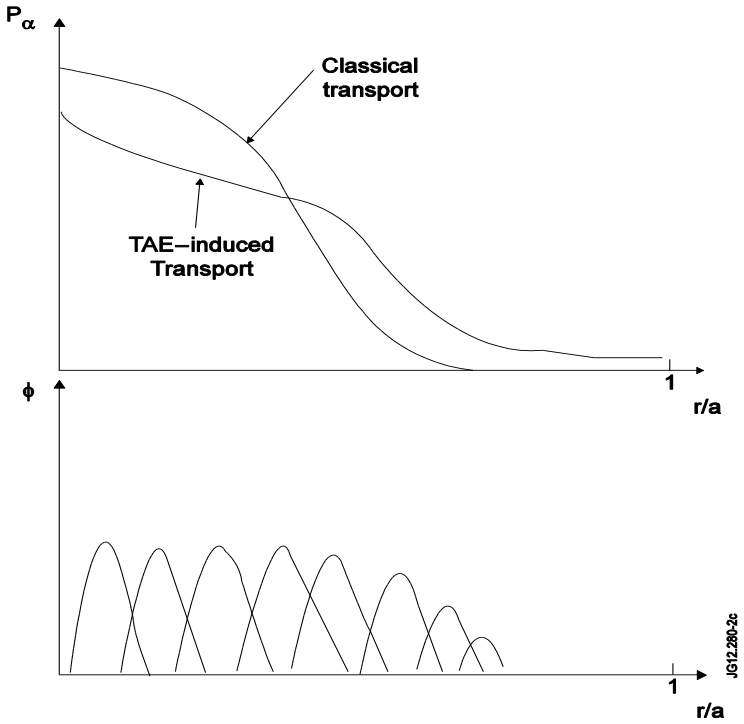

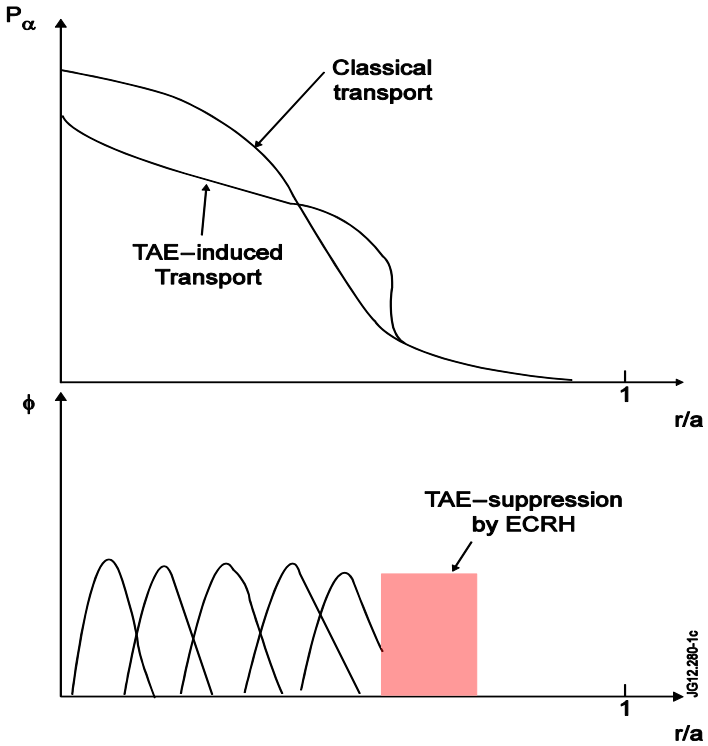

ECRH/ TAE EXPERIMENTS ON AUG (2014-2016)

S E Sharapov et al 2018 Plasma Phys. Control. Fusion 60 014026

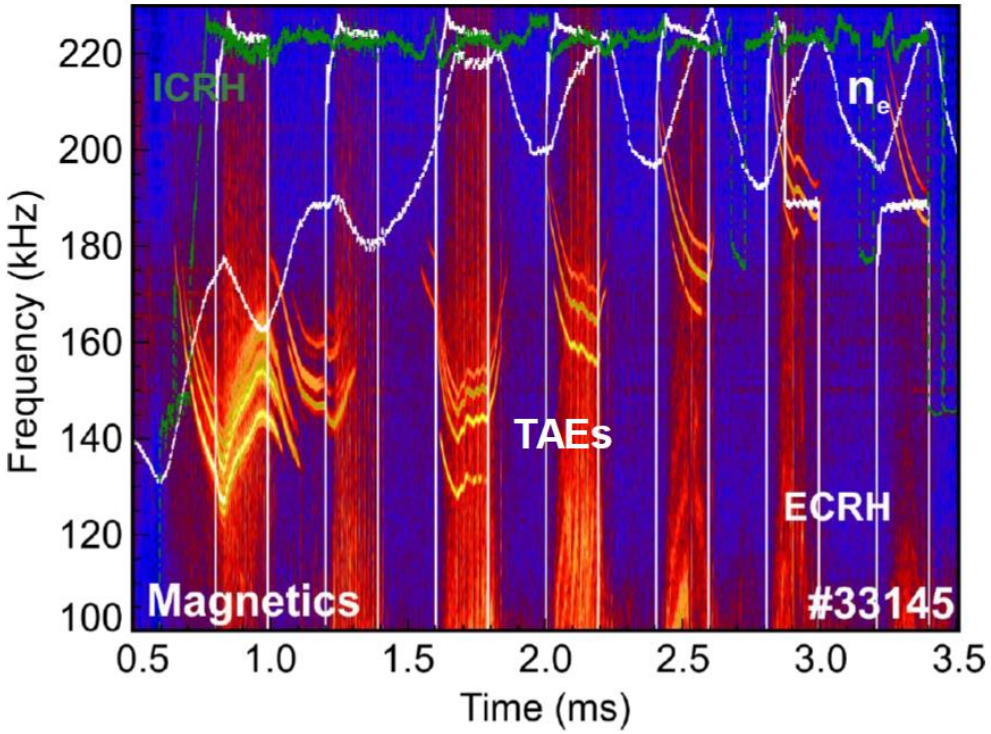

- **TAE frequency sweeps down fast as plasma density increases**
- **Facilitation of TAE instability due to off-axis ECRH was observed!**

SLOWING-DOWN TIME AND W_{fast} INCREASE DURING ECRH

SELFO results for AUG #33150, from 2.0 s to 2.6 s:

- **Up to ~40% higher fast ion energy content W_{fast} with ECRH applied off-axis;**
- **Strong correlation between W_{fast} and TAE activity;**
- **W_{fast} increases due to longer slowing-down time;**
- **Fast ion pressure gradient is significantly higher with ECRH when TAEs appear.**

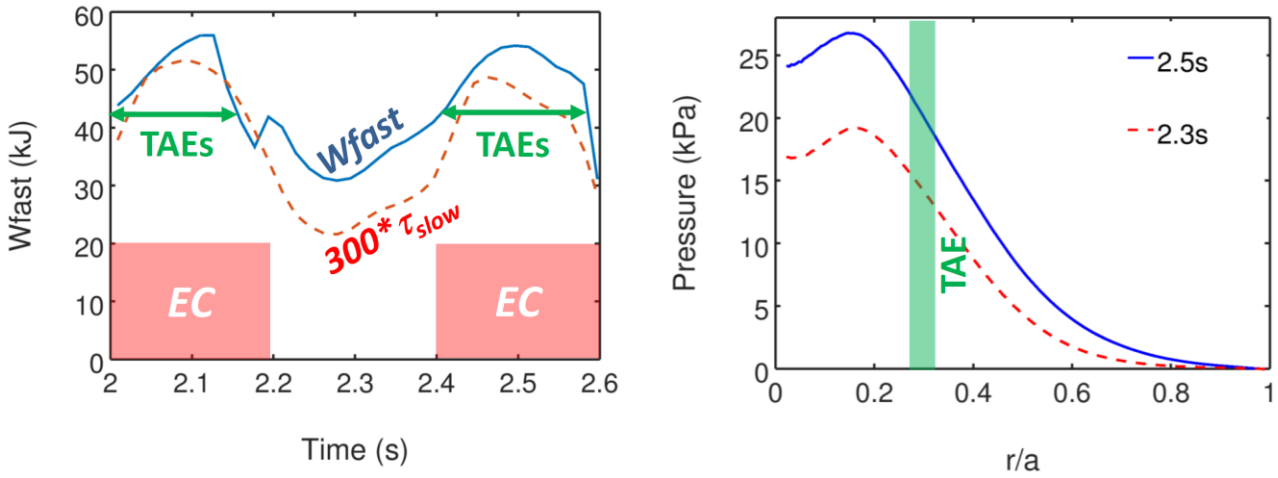

COMING TO CURRENT DRIVE NOW: ECCD/ TAE EXPERIMENT ON AUG (30 June 2020)

- **Excite TAEs with ICRH-accelerated ions at P_{ICRH}=const;**
- **Apply ECCD at ~ρ_{TAE}, vary P_{ECCD}, find threshold for TAE stabilization;**

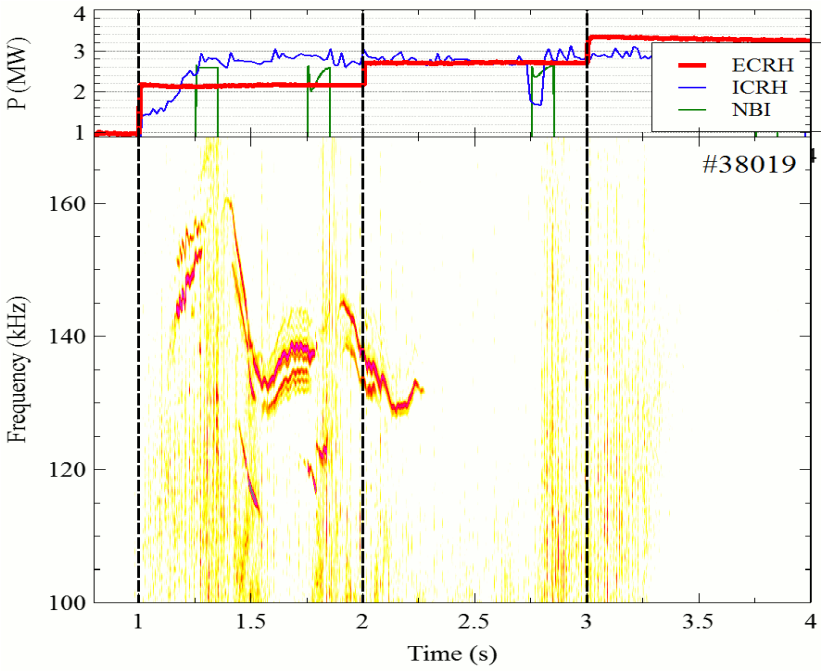

SUMMARY ON ECCD/TAE RESULTS OBTAINED:

a)38017 Counter-ECCD
b)38012 Reference ECRH
c)38018 Co-ECCD

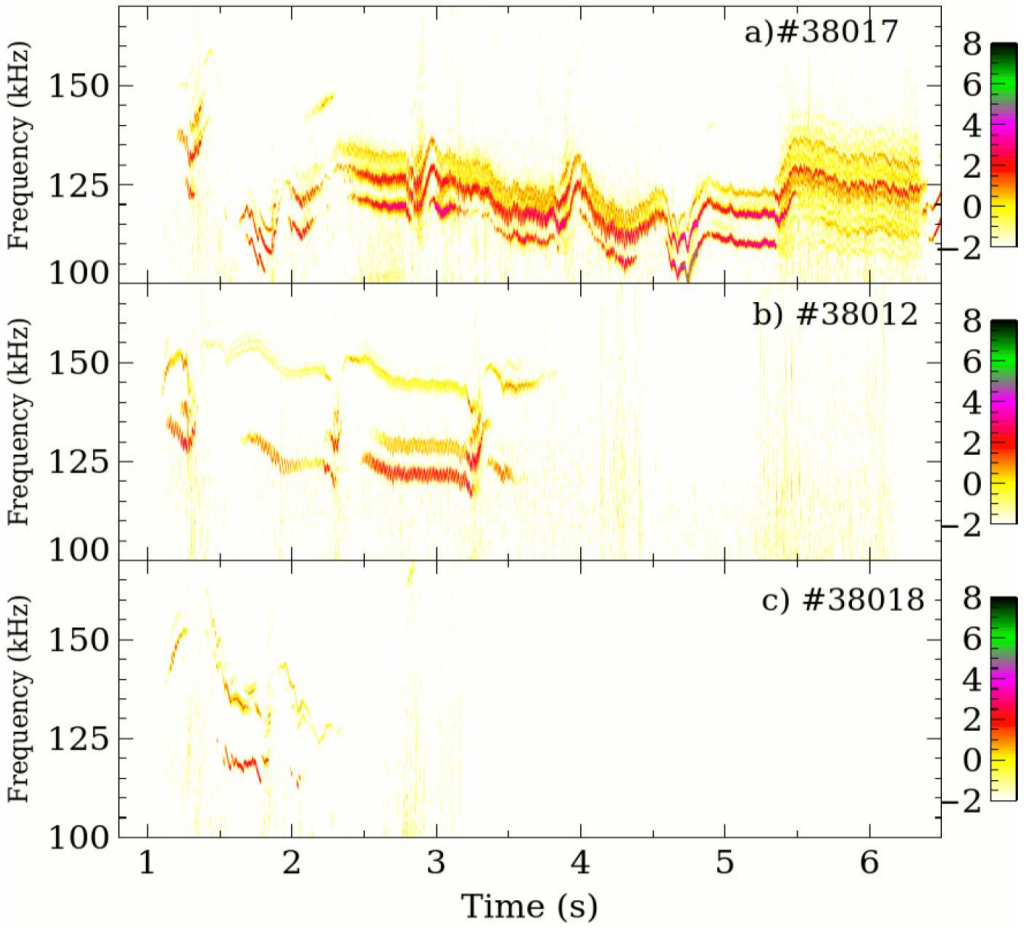

SUMMARY ON ECCD/TAE EXPERIMENT ON AUG – cont'd

- **4 comparison discharges were performed on AUG:**
- **#38012 (ECRH Reference)**

  #38017 (Counter-ECCD)
  #38018 (Co-ECCD)
  #38019 (Co-ECCD, smaller steps in P_{ECCD})

- **Two branches of TAEs were identified residing at ρ~0.4 (f~125 kHz) and ρ~0.6 (f~150 kHz), #38012**

- **Counter-ECCD at ρ~0.5 suppressed TAEs at ρ~0.4 (f~150 kHz), but greatly amplified and prolonged to ~6.5 s TAEs at ρ~0.6 (f~125 kHz), #38017**

- **Co-ECCD applied also at ρ~0.5, but with a broader deposition profile suppressed ALL TAEs at P_{ECCD} > 2.7 MW, #38018, 38019.**

TAE SUPPRESSION IS DUE TO CONTINUUM DAMPING INCREASE

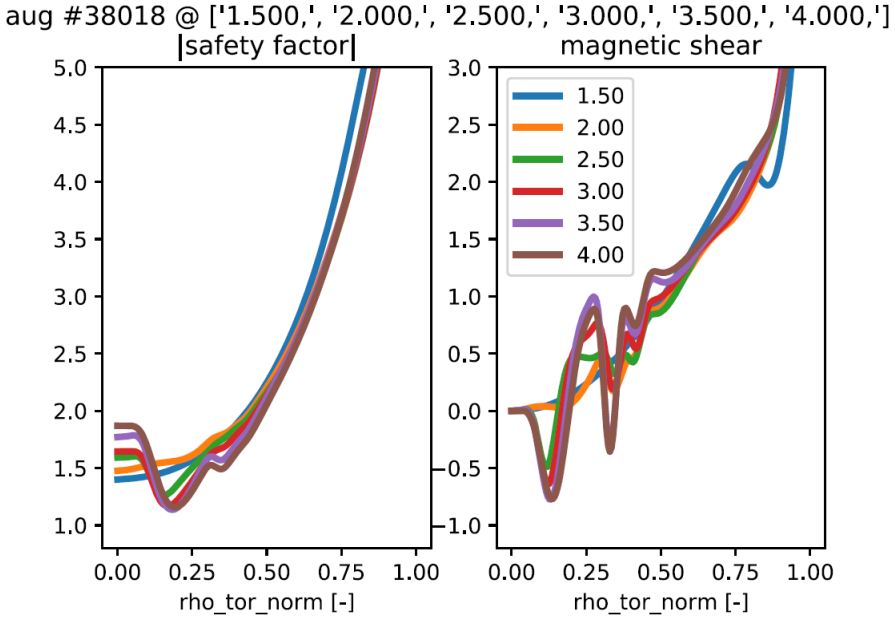

#38018 (co ECCD)

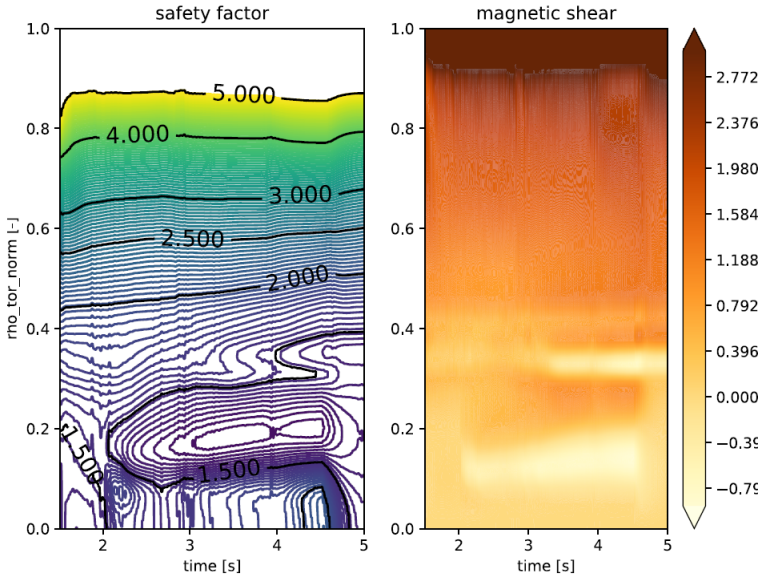

SUPPRESSION OF NBI-DRIVEN MODES BY ICRF AT HIGH HARMONIC ON NSTX-U

High Harmonic Fast Wave suppression of both TAE and GAE

- TAE and GAE excited with 2MW of NBI heating.
- Both TAE and GAE reappear shortly after HHFW heating ends.
- HHFW, primarily for heating thermal electrons, also heats beam ions.
- Heating affect similar to energy diffusion – should suppress chirping.
- However, modes appear completely stabilized.

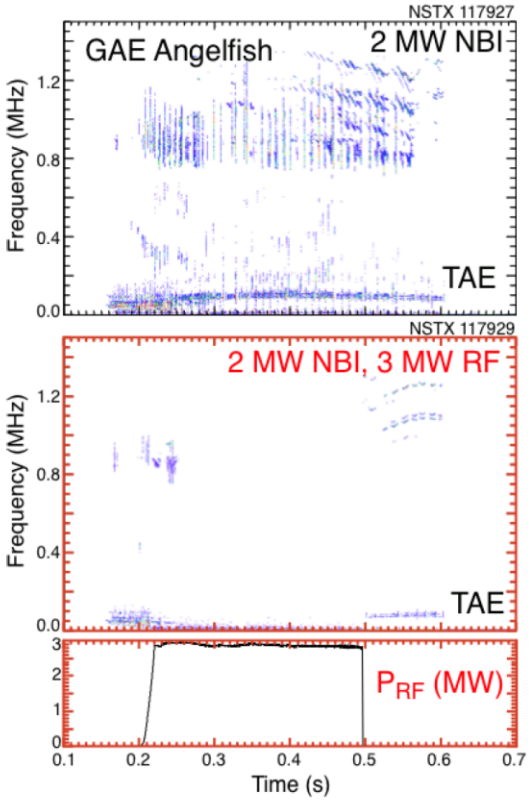

E.Fredrickson et al. ,18th Workshop MHD Control, Santa Fe, New Mexico, 2013

An alternate explanation to enhanced diffusivity is that the HHFW depletes the resonant fast ions

- Modes are excited through Doppler-shifted cyclotron resonance

  $\omega_{ci} = \omega_{mode} + k_{||} V_{b||}$

- Indicated by red (initial frequency) and blue (final frequency) curves,
  - most likely the resonant fast ions are on stagnant orbits
- HHFW will increase perpendicular energy, reducing drive for modes.

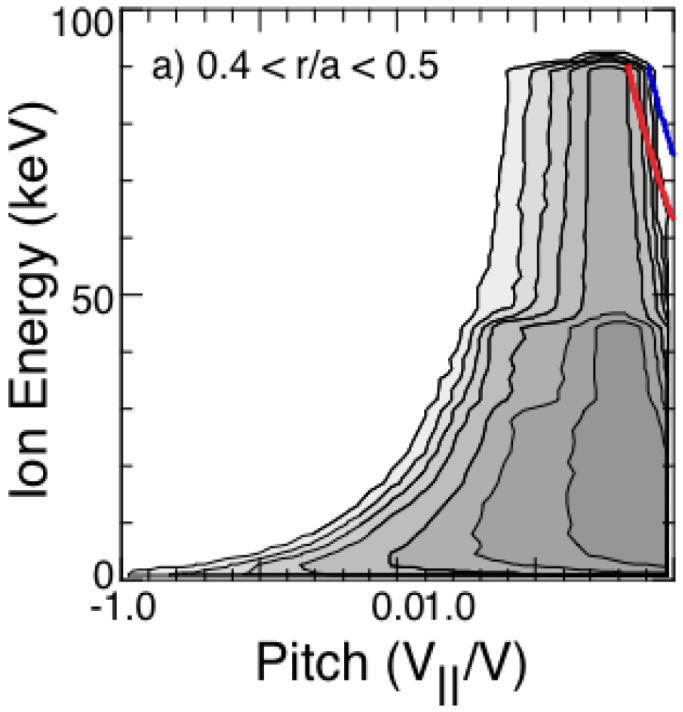

SUMMARY

Control of EP and EP-driven instabilities is a real challenge in burning plasma with high Q

Possible EP radial gradient control with toroidally-propagating ICRH and with externally applied static 3D fields were established

Mitigation of AEs in reversed-shear configurations with ECRH applied at q_{min} became mature up to the level of real-time control

ECRH was found to facilitate TAEs on AUG

ECCD was found to do "anything" on AUG depending on the directivity

Suppression of NBI-driven AEs with HHFW was demonstrated on NSTX-U